



HAL
open science

Simulating local adaptation to climate of forest trees with a physio-demo-genetics model

Sylvie Oddou-Muratorio, Hendrik Davi

► **To cite this version:**

Sylvie Oddou-Muratorio, Hendrik Davi. Simulating local adaptation to climate of forest trees with a physio-demo-genetics model. *Evolutionary Applications*, 2014, 7 (4), pp.453-467. 10.1111/eva.12143 . hal-01065117

HAL Id: hal-01065117

<https://hal.science/hal-01065117>

Submitted on 28 May 2020

HAL is a multi-disciplinary open access archive for the deposit and dissemination of scientific research documents, whether they are published or not. The documents may come from teaching and research institutions in France or abroad, or from public or private research centers.

L'archive ouverte pluridisciplinaire **HAL**, est destinée au dépôt et à la diffusion de documents scientifiques de niveau recherche, publiés ou non, émanant des établissements d'enseignement et de recherche français ou étrangers, des laboratoires publics ou privés.

1 **Title: Simulating local adaptation to climate of forest trees with a Physio-**

2 **Demo-Genetics model**

3

4 **Authors:** Sylvie Oddou-Muratorio^{1*}, Hendrik Davi^{1*}

5 **Both authors contributed equally to this work*

6 **Adresses:**

7 ¹ INRA, UR629 Ecologie des Forêts Méditerranéennes (URFM), F-84914 Avignon, France

8 **e-mails:** oddou@avignon.inra.fr; hendrik.davi@avignon.inra.fr

9 **Running head:** Physio-Demo-Genetic model for trees

10 **Acknowledgments:** We thank K Csilléry, M. Cailleret, E Klein, F Lefèvre, O. Savolainen

11 and two anonymous reviewers for useful comments on a previous version of this manuscript.

12 We are indebted to F de Coligny, P. Dreyfus, C. Pichot for the informatics development on

13 CAPSIS. We thank A. Amm, A Bontemps and M Cailleret, J Gauzère for their PhD studies

14 that allowed the calibration of PDG. This calibration benefitted from the support of UEFM (F

15 Jean, O Gilg, M Pringarbe, F Rei, N Turion). The development of the PDG model was funded

16 by FRB (VARIADAPT), ERANET Linktree and ERANET Tiptree. Simulations were

17 performed on the computation cluster of INRA BioSp, Avignon.

18 **Type:** Original Research article

19

20

21 Abstract

22 One challenge of evolutionary ecology is to predict the rate and mechanisms of population
23 adaptation to environmental variations. The variations in most life-history traits are shaped
24 both by individual genotypic and environmental variation. Forest trees exhibit high levels of
25 genetic diversity, large population sizes, and gene flow, and they also show a high level of
26 plasticity for life-history traits. We developed a new Physio-Demo-Genetics model (denoted
27 PDG) coupling (1) a physiological module simulating individual tree responses to the
28 environment; (2) a demographic module simulating tree survival, reproduction and pollen and
29 seed dispersal; and (3) a quantitative genetics module controlling the heritability of key life
30 history traits. We used this model to investigate the plastic and genetic components of the
31 variations of the timing of budburst along an elevational gradient of *Fagus sylvatica* (the
32 European beech). We used a repeated five years climatic sequence to show that five
33 generations of natural selection were sufficient to develop non-monotonic genetic
34 differentiation in the timing of budburst along the local climatic gradient but also that plastic
35 variation among different elevations and years was higher than genetic variation. PDG
36 complements theoretical models and provides testable predictions to understand the adaptive
37 potential of tree populations.

38 Key words: individual-based model, quantitative genetics, ecophysiology, budburst
39 phenology, quantitative trait loci, European beech, *Fagus sylvatica*

40

41 Introduction

42 The ongoing and predicted rapid changes in temperature, precipitation and CO₂ atmospheric
43 concentration and the resulting increase in the frequency and intensity of extreme events such
44 as droughts will have a wide range of long-term implications for natural population dynamics
45 and ecosystem sustainability. Within a population, these changes impose strong selective
46 pressures, which affect demographic rates and can cause genetic evolution across generations
47 (Hansen *et al.*, 2012). Moreover, Climate Change (CC) also affects the physiology and
48 development of individual organisms up to the limits of their phenotypic plasticity, i.e. the
49 ability of individual genotypes to produce alternative phenotypes in different environments
50 (Chevin *et al.*, 2013). The interplay between genetic evolution and phenotypic plasticity
51 ultimately determines a population's ability to adjust (without migrating) to novel
52 environmental conditions imposed by CC. Investigating these mechanisms is essential for
53 predicting eco-evolutionary dynamics and ecosystem services and for guiding conservation
54 efforts.

55 This issue is crucial for trees because of their pivotal role in the functioning and biodiversity
56 of forest ecosystems. Multi-site experiments (using forester provenance tests) showed that
57 current tree populations can adjust to varying environmental conditions through phenotypic
58 plasticity over a non-negligible latitudinal range (Rehfeldt *et al.*, 2002). Moreover, based on
59 the patterns of local adaptation displayed by most tree species over the course of post-glacial
60 recolonization, forest tree populations are usually assumed to have a high evolutionary
61 potential (Alberto *et al.*, 2013; Savolainen *et al.*, 2007); however, tree population abilities of
62 genetic evolution over a short timescale (i.e., microevolution) remain largely unresolved. In
63 addition, plasticity and genetic adaptation can interact together and with gene flow, as
64 illustrated mostly by theoretical models or studies of model species. One well-known
65 interaction is the interplay between gene flow and adaptation when the environment changes

66 both in space and time {Polechová, 2009 #1054}. Trees are capable of long-distance pollen-
67 mediated gene flow, which could promote adaptive evolution to novel environments (Kremer
68 *et al.*, 2012). Another pervasive interaction involves plasticity and genetic adaptation;
69 plasticity can be adaptive if plastic trait variation increases individual fitness (Nicotra *et al.*,
70 2010), or it can be maladaptive if plasticity decreases fitness (Ghalambor *et al.*, 2007).
71 Moreover, when adaptive plasticity cannot evolve, it can slow down the genetic response to
72 directional selection, but it also allows phenotypes to track environmental change more
73 closely (Chevin *et al.*, 2013).

74 Methodological developments currently limit our understanding of the interplay among
75 plasticity, genetic adaptation and gene flow and their impacts on tree population dynamics. In
76 most evolutionary models thus far developed for tree life history traits, individual fitness is
77 either directly controlled by the genotype (Le Corre & Kremer, 2003) or derived from
78 genetically controlled life history traits (Kuparinen *et al.*, 2010). Climate effects on water and
79 carbon exchanges is a complex process that has been studied by eco-physiologists and has
80 rarely been explicitly taken into account as a selective pressure in evolutionary models (but
81 see (Kramer *et al.*, 2008). Similarly, the inter-individual variation and adaptive potential of
82 traits related to climate response have rarely been incorporated into biophysical and eco-
83 physiological models.

84 The different time scales considered by eco-physiological and evolutionary models (typically
85 from the hour to the year or tens of years for the former versus many generations at
86 equilibrium for the latter) are generally considered to be challenges in the development of
87 coupled physio-genetic models. However, neither of these time scales may be relevant for
88 forming accurate predictions of realistic tree population responses to CC. Indeed, current
89 forest tree populations can rarely be considered to be at equilibrium, and demographic
90 processes play a major role in the dynamics of adaption over a few generations (Savolainen *et*

91 *al.*, 2007). Moreover, CC is likely to involve non-continuous and non-predictable change in
92 response to abiotic conditions, which limit the relevance of long-term predictions at
93 equilibrium (Kremer & Le Corre, 2011). In contrast, the predictions of biophysical and eco-
94 physiological models cannot be generalized over more than one generation if the
95 microevolution of functional traits within a population is not negligible. Therefore, there is a
96 need for physio-genetic models to address the timescale of a few generations (<10).

97 In the present study, we propose a new Physio-Demo-Genetics model (PDG) coupling the
98 following: (1) a functional module derived from CASTANEA (Dufrêne *et al.*, 2005) to
99 simulate carbohydrate and water fluxes at the tree level using daily climate observations; (2) a
100 population dynamics module to convert carbohydrate reserves into demographic rates for
101 adult trees (growth, mortality and seed production) and to simulate ecological processes
102 across the life cycle (including seed and pollen dispersal, germination rate and density-
103 dependent mortality of seedlings); and (3) a quantitative genetics module relating genotype of
104 the quantitative trait loci (QTL) to the phenotype of one or more functional traits (Labonne &
105 Hendry, 2010). This individual-based, spatially explicit model simulates the evolution of
106 functional traits in tree populations, where phenotypic differences between individuals are
107 determined by their genotype at QTLs that control functional traits and by their physiological
108 response to local climate conditions. PDG is available from the CAPSIS modeling platform
109 (Dufour-Kowalski *et al.*, 2012).

110 We used PDG to simulate local adaptation in a continuous tree population that expands along
111 an elevational gradient based on experimental data collected from *Fagus sylvatica*
112 populations on Mont Ventoux in southeastern France. Under divergent selection, local
113 adaptation is expected to result in phenotypic differentiation for traits contributing to fitness
114 across the gradient. Among the various traits contributing to fitness, we focused on the timing
115 of budburst (TBB), a phenological trait that determines the length of the growing season in *F.*

116 *sylvatica* (Davi *et al.*, 2011). An earlier budburst extends the time during which
117 photosynthesis occurs (Richardson *et al.*, 2006), but it also increases the risk of late frost
118 damage (Dittmar & Elling, 2006). *In situ* observations of *F. sylvatica* on Mont Ventoux
119 revealed a classical phenotypic cline in TBB resulting from plastic variation; budburst occurs
120 earlier at lower than higher elevations because TBB is triggered by the heat sum (Davi *et al.*,
121 2011). The opposite is observed for genetic clines as assessed in common garden
122 experiments, where TBB is observed under the same environmental conditions for all
123 populations; under such conditions, *F. sylvatica* populations originating from higher
124 elevations show earlier budburst than those originating from lower elevations (Gomory &
125 Paule, 2011; Vitasse *et al.*, 2009a; von Wuehlisch *et al.*, 1995). This situation in which the
126 phenotypic and genetic clines vary in opposite directions is referred to as a counter-gradient
127 variation. In contrast, genetic and phenotypic clines have been shown to exhibit co-gradient
128 variation for TBB in some species (e.g., *Quercus sp.*), while clear linear genetic clines are not
129 observed for other species (e.g., *Fraxinus*) (Vitasse *et al.*, 2009a).

130 In this paper, we illustrate the potential of PDG to elucidate the processes through which
131 adaptation proceeds for *Fagus sylvatica* on Mont Ventoux. We address the following issues:
132 (1) How do adaptive genetic variation and phenotypic plasticity contribute to TBB variation
133 along an elevational gradient? (2) How fast can genetic differentiation in TBB develop? (3) Is
134 there a monotonic trend in the genetic variation across the gradient?

135 **Materials and Methods**136 *Overview of PDG model*137 *The physiological process-based module*

138 This module corresponds to the CASTANEA library hosted on the Capsis platform. Initially
 139 developed at the stand scale, CASTANEA (Dufrêne *et al.*, 2005) simulates canopy
 140 photosynthesis (i.e., Gross Primary Production, GPP) and transpiration, maintenance and
 141 growth respiration, seasonal development and assimilate partitioning to leaves, carbohydrate
 142 storage (hereafter reserves), stems, branches and coarse and fine wood. The meteorological
 143 driving variables are global radiation, rainfall, wind speed, air humidity and temperature. A
 144 complete description of the model is given in Dufrêne *et al.* (2005), and the sub-model of
 145 carbon allocation is described by (Davi *et al.*, 2009).

146 In its initial version, CASTANEA simulated CO₂ and H₂O fluxes, considering one average
 147 tree as representative of the whole stand. To account for inter-individual variation, we
 148 considered each tree as a single unit with its own parameters for the CASTANEA simulation.
 149 Note that all CASTANEA units were treated independently, meaning that we do not account
 150 for competition among trees for light or soil water acquisition. In contrast with the stand-level
 151 version, we computed several variables at the individual tree level, including biomass (B_{tree}),
 152 leaf area index (LAI) by tree and crown projection (A_{crown}), to determine the carbon and water
 153 budgets of each tree (see online Appendix 1).

154 Only one out of all the CASTANEA parameters was allowed to vary among trees, namely,
 155 F_{critBB} , the critical value of the state of forcing, which is most commonly referred to as the
 156 temperature sum required for budburst. The timing of budburst (TBB) was simulated
 157 following the equations 1-3:

$$158 \quad R_{ficBB} = \begin{cases} T - T_2 & \text{if } T > T_2 \text{ and } N > Nstart1 \\ 0 & \text{if } T \leq T_2 \text{ or } N < Nstart1 \end{cases} \quad (1)$$

159 where R_{frcBB} is the rate of forcing for bud break, T the mean daily temperature, T_2 the base
 160 temperature, N the day of year and N_{START1} the date of onset of rest.

$$161 \quad S_{\text{frcBB}} = \sum_{N_{\text{START1}}}^N R_{\text{frcBB}} \quad \text{if} \quad S_{\text{frcBB}} < F_{\text{critBB}} \quad (2)$$

$$162 \quad \text{TBB} = N \quad \text{if} \quad S_{\text{frcBB}} \geq F_{\text{critBB}} \quad (3)$$

163 with S_{frcBB} the state of forcing, F_{critBB} the critical value of state of forcing for the transition
 164 from quiescence to the active period and TBB the day when bud break occurred.

165 We chose to focus on the F_{critBB} variation for two reasons. First, F_{critBB} is one of 17 key
 166 parameters according to the sensitivity analyses performed in Dufrêne *et al.* (2005). Second,
 167 the genetic clines observed for TBB in a common garden of populations from different
 168 elevations are likely to result from among-population variation for F_{critBB} . For the sake of
 169 simplicity, we assumed that the effect of chilling on dormancy was constant across year and
 170 elevations.

171 To assess the impact of drought on photosynthesis, an annual water stress index (WSI) was
 172 estimated at the tree level as the sum of the daily reduction of photosynthesis caused by soil
 173 drought (i.e., when the relative soil water content drops below 40% of the soil water reserve).

174 In this version of CASTANEA, we also added the effect of late frost on LAI. Trees are most
 175 sensitive to frost during budburst; frost can kill the new shoots, reduce growth and cause
 176 misshapen branching (Dittmar & Elling, 2006). When unfolding leaves are affected by frost,
 177 decreased leaf area is expected. In PDG, every day during which the minimal daily
 178 temperature (T_{min}) fell below a threshold value ($T_{\text{minEffect}}$) following the initiation of budburst
 179 was considered to affect the leaf area index (LAI) as follows:

$$180 \quad LAI_{\text{tree}}(\text{day} + 1) = LAI_{\text{tree}}(\text{day}) \left(1 + (T_{\text{minEffect}} - T_{\text{min}}) \text{Coef}_{\text{FrostEffect}} \right) \quad (4)$$

181 *Parameterization:* In previous studies, species-specific CASTANEA parameters for *F.*
182 *sylvatica* were determined and CASTANEA was validated at an experimental site in Northern
183 France (Davi *et al.*, 2005). Additionally, some site-specific parameters were measured in
184 Ventoux (Table 1). First, the budburst model was calibrated using two types of data. The
185 onset date of rest (R_{fcBB}) was estimated by an experiment on dormancy release in the spring
186 of 2012 (unpublished data). The average critical value for the state of forcing (F_{critBB}) was
187 estimated by using budburst survey from 2007 to 2011 at two elevations (1117 and 1340 m)
188 for 20 trees per elevation (Fig. 1). Characteristics of sun leaves (nitrogen content and
189 LMA=leaf mass per area) were obtained for 149 trees in an intensive-studied plot (Bontemps,
190 2012). Canopy clumping (CI) was estimated by using five hemispherical photographs taken in
191 the same plot in the summer of 2008, following the methodology described in Davi *et al.*
192 (Davi *et al.*, 2008). The photosynthesis parameter (maximum carboxylation rate=51.6 μmol
193 $\text{photon m}^{-2} \text{s}^{-1}$) was estimated from previous measurements at the same site in the summer of
194 2006 (Ducrey & Huc, pers. comm.).

195 *The demographic module*

196 *Adult growth, mortality and seed production:* The reserves produced by photosynthesis at a
197 daily time step were allocated to growth and used to predict tree mortality. Two levels of
198 carbon reserves were considered: the carbon reserve at the end of the year (CumCR; Table 1)
199 and the difference between the carbon reserves before budburst and the amount of carbon
200 required for the complete development of new leaves (bbCR; Table 1). Below a critical level
201 of one of these two indicators, a tree would die. Critical levels of CumCR and bbCR were
202 estimated based on mortality rates assessed on Mount Ventoux (Davi unpublished results).

203 Biomass allocated to wood between the date of budburst and leaf senescence was converted
204 into a diameter at breast height (DBH) increment. Finally, at the end of the year, if the

205 biomass of accumulated reserves (B_{res}) exceeded the critical rate for seed production (sB_{res}),
 206 the reserve was converted into primary seed production (N_S) for each tree as follows:

$$207 \quad N_S = C_P R_{SP} \left(\frac{B_{res} - sB_{res}}{c} \right) \quad (5)$$

208 where C_P is the crown projection of the tree (online Appendix 1), R_{SP} is the rate of seed
 209 production (Table 1) and c is the cost to produce one seed. Parameter c was estimated by
 210 using the dry mass and carbon content of seeds and cupules (Han *et al.*, 2011) assuming an
 211 associated respiratory cost of 50%.

212 The effective seed production of a tree, that is, its female fecundity, was computed as
 213 follows:

$$214 \quad F = N_S (1 - r_{ES}) r_{SS} r_{SG} \quad (6)$$

215 where r_{ES} is the rate of empty seeds, r_{SS} is the rate of seed survival and r_{SG} is the rate of
 216 seed germination. Parameters r_{ES} and r_{SG} were calibrated on the basis of a germination
 217 experiment in the years 2009-2010, during which 60 seed lots were collected at three
 218 elevational levels from Mont Ventoux (20 mother trees per altitude level), and from 100 to
 219 300 seeds/mother tree were scanned (to measure the r_{ES}) and sown after stratification (to
 220 measure the r_{SG}).

221 *Pollen dispersal and mating:* Pollen dispersal was modeled by an exponential dispersal kernel
 222 describing the probability that a pollen grain emitted at position (0,0) would pollinate a seed-
 223 tree at distance r as follows:

$$224 \quad p_P(a_P, r) = \frac{1}{2\pi \cdot a_P^2} \exp\left(-\frac{r}{a_P}\right) \quad (7)$$

225 where the scale parameter a_P is homogeneous to the mean distance traveled by pollen grain
 226 (δ_P) with the relationship $\delta_P = 2a_P$ (Table 1). The simulation domain was defined with
 227 reflecting borders to avoid the loss of border tree progeny.

228 The contribution π_{jk} of pollen-tree k to the outcrossing pollen cloud to the fertilization
 229 of seed tree j ($j \neq k$) depended on the distance between trees j and k through the pollen dispersal
 230 kernel p_P and on its pollen fecundity as related to the diameter DBH_k as follows:

$$231 \quad \pi_{jk} = p_P(a_P, b_P) \times e^{\gamma_m DBH_k} \quad (8)$$

232 where γ_m is related to the diameter effects on male fertility. We assumed no pollen limitation.
 233 In addition to outcrossing, selfing was considered to occur at a fixed rate s . Tree j was self-
 234 pollinated with probability s ; and pollinated by other individuals with probability $(1-s) \pi_{jk}$ (for
 235 $1 \leq k \leq N$ and $k \neq j$), where N is the total adult population size. Parameters δ_P , s and γ_m were
 236 estimated for the *F. sylvatica* trees on Mont Ventoux ((Oddou-Muratorio *et al.*, 2010).

237 *Seed dispersal and recruitment (density-dependent mortality):* The simulation domain was
 238 divided in squared cells to model seed dispersal. The intensity of seed rain from a given seed
 239 tree j on the center of cell i was expressed by

$$240 \quad \tau_{ij} = p_S(a_S, r_{ij}) F_j \quad (9)$$

241 where p_S is the seed dispersal kernel, r_{ij} is the distance from tree j to the center of cell i and F_j
 242 is the female fecundity of seed tree j . The seed dispersal kernel was modeled as pollen
 243 dispersal by using the exponential kernel described by equation 4. From τ_{ij} , we computed the
 244 number of new trees N_{ij} from a given seed tree j on the whole cell i of area S , as detailed in
 245 online Appendix 2.

246 Within each cell i , $\sum_j N_{ij}$ individuals ($j=1$ to the total number of seed trees) were created at the
 247 age of 40 years, thus assuming that the phenology selection did not proceed differently before
 248 and after this life stage. The height and diameter of newly created trees were drawn in a
 249 Gaussian distribution of parameter $\{\mu_H; SD_H\}$ and $\{\mu_{DBH}; SD_{DBH}\}$, respectively. The spatial
 250 position of each new tree was allocated randomly within the cell unless its mother tree was in

251 the same cell i ; in this case, spatial positions were drawn in a Gaussian dispersal kernel
252 around the position of the mother tree. Mortality during recruitment was modeled as a spatial,
253 random (i.e., independent from TBB), density-dependent process considering that no tree
254 pairs could have more than 30% overlapping crown.

255 *A quantitative genetic module for the timing of budburst (TBB)*

256 The variation of TBB between individuals depended on both (1) the individual genetic
257 variation in F_{critBB} and (2) environmental variation among individual locations and years. In a
258 given environment, the higher is the F_{critBB} , the later is the TBB. In most of the simulated
259 scenarios, the environmental component of TBB variation was fully determined by the
260 variation in daily temperatures during the spring, which varied across years for a given
261 individual, and across elevations for different individuals. Note that in our simulations,
262 elevation could vary by 200 m between individuals within the same population (see paragraph
263 “Simulation result analyses” below), and thus both the variation in F_{critBB} and elevation
264 contribute to the variation in TBB within population.

265 The value of F_{critBB} was determined by ten independent biallelic loci with purely additive
266 effects. The occurrences of mutations and new allele immigration from other populations than
267 those simulated were ignored. The contribution of a genotype at a given locus l to F_{critBB} was
268 given as $m_l + \alpha_l$, m_l and $m_l - \alpha_l$ for the homozygote $A1A1$, the heterozygote $A1A2$ and the
269 homozygote $A2A2$, respectively. All the m_l 's were identical and equal to $\mu_{F_{critBB}}/10$ (Table S1).
270 We followed the method proposed by Bost et al. (2001) to generate the distribution of allelic
271 effects. They showed that for N_l loci having an equal $m_l = \mu/N_l$ contribution to the trait, an L-
272 distribution of QTL effects could be simulated with allele effects randomly drawn from a
273 Gaussian distribution of mean $\mu/2N_l$ and with a standard deviation σ small enough to ensure
274 that α_l belongs to $[0; \mu/L]$ (here, $\sigma = \mu/8N_l$). Allelic effects α_l were constant over time (Table

275 1). The genetic variance for F_{critBB} within the population/subpopulation was computed as
276 follows: $V_A = \sum_l 2p_l(1-p_l)\alpha_l^2$, where p_l is the frequency of allele A1 at locus l .

277 In most scenarios with microevolution, we considered F_{critBB} to be fully heritable; the narrow-
278 sense heritability h^2_{NS} of F_{critBB} was set to 1, meaning that the phenotypic variance of F_{critBB}
279 (V_P) equaled to the additive genetic variance V_A (as $h^2_{NS}=V_A/V_P$), and that the environmental
280 variance V_E was 0. Each individual F_{critBB} -value was the sum of genotypic contributions (see
281 above) across the 10 loci. In the control scenario, F_{critBB} was variable but not heritable (i.e.
282 $V_A=0$); to match the phenotypic variation obtained in micro-evolution scenarios, V_P was set to
283 $V_E=22$. Individual F_{critBB} -values were randomly drawn from a Gaussian distribution of mean
284 $\mu_{F_{critBB}}$ and of variance V_P . Finally, we also considered the case where F_{critBB} was itself a
285 quantitative trait with $h^2_{NS}=0.6$ (Kramer et al. 2008); each individual F_{critBB} -value was the sum
286 of an additive genetic component and of a stochastic environmental component, drawn in a
287 Gaussian distribution of mean 0 and of variance V_E , so that $V_E=(1-h^2_{NS})V_P$ and $V_A=22$.

288 **Simulation design and testing hypothesis**

289 We applied PDG to simulate the evolutionary dynamic of *F. sylvatica* along an elevational
290 gradient from 700 to 1700 m on a 20 ha grid (200 m x 1000 m) divided into 500 cells (20 m x
291 20 m) (Fig. 2). This case study mimic an elevational gradient located on Mont Ventoux
292 (southeastern France, 44°10'28''N; 5°16'16''E), where *F. sylvatica* recently expanded under
293 the black pines (*Pinus nigra*) that were planted at the end of the 19th century. The species
294 currently extend from 750 to 1700 m in elevation on the northern aspect. Environmental,
295 climatic and ecological data were available from previous studies (Cailleret & Davi, 2011;
296 Davi et al., 2011).

297 *Initial conditions and neutral pre-evolution*

298 The initial population included 500 trees (all 40 years old). Their initial height and diameter
299 were drawn by following a Gaussian distribution with parameters $\{\mu_H; SD_H\}$ and $\{\mu_{DBH};$
300 $SD_{DBH}\}$ (Table 1). Initial allele frequencies were drawn from a uniform distribution [0,1], and
301 they formed genotypes according to the Hardy-Weinberg equilibrium. The initial population
302 was split into five equal sub-populations at the following five elevational ranges: 790-810 m,
303 990-1010 m, 1190-1210 m, 1390-1410 m and 1590-1610 m (Fig. 2). To introduce initial
304 genetic differentiation among sub-populations and spatial genetic structure within sub-
305 populations similar to the levels observed on the field, we first simulated five generations
306 without selection in which the allelic frequencies within and among subpopulations evolved
307 only as a result of genetic drift and gene flow (online Appendix 3).

308 *Adaptive evolution over six generations*

309 After initialization, we simulated six non-overlapping generations (from G_0 to G_5) of
310 evolution with selection in addition to genetic drift and gene flow. Selection occurred within
311 each generation both through differential mortality and differential reproduction of individual
312 trees. Each generation lasted 70 years and included (1) a seedling stage (from years/ages 0 to
313 39) and (2) an adult stage (from years/ages 40 to 70). Adult trees grew for 20 years without
314 reproducing (i.e., until age 60) and then grew and reproduced over the course of ten years.
315 After 70 years, all the surviving trees were removed. Seeds produced during generation G_x
316 were sent into dormancy until the beginning of generation G_{x+1} , when survival depended on
317 the total seedling density.

318 *Climatic data*

319 The basis climate variables (X_{basis}) were assessed from 2002 to 2006 by using daily
320 meteorological data measured at a permanent weather station located in Ventoux (Porté *et al.*,
321 2004). The elevation effects on temperature, relative humidity and precipitation were

322 estimated by using linear models and data acquired from April 2007 to October 2009 using
 323 five HOBO Pro V2 microloggers, which were located at 995, 1117, 1225, 1340 and 1485 m
 324 on the north face (Cailleret & Davi, 2011), as follows (Table S2):

$$325 \quad T(z) = \varphi_1 T_{\text{basis}} + \varphi_2 z + \varphi_3 \quad (10) \text{ for temperatures}$$

$$326 \quad RH(z) = (\chi_1 + \chi_2 z) RH_{\text{basis}} + \chi_3 \quad (11) \text{ for relative humidity}$$

$$327 \quad P(z) = (\psi_1 + \psi_2 z) P_{\text{basis}} \quad (12) \text{ for precipitation}$$

328 This five-year climate sequence (from 2002 to 2006) was repeated in loops (six loops) for 30
 329 years at each generation.

330 *Testing of hypotheses*

331 The present study investigated how phenotypic plasticity and genetic adaptation contributed
 332 to TBB variation across elevations by comparing the following scenarios:

- 333 – Scenario **A (“Neutral”)** was the baseline scenario without adaptive evolution, because
 334 F_{critBB} was variable but not heritable ($h^2=0$). Selection occurred within a generation but
 335 was not expected to result in F_{critBB} changes between generations.
- 336 – Scenario **B (“Adaptive evolution”)**, in which F_{critBB} was variable and heritable ($h^2=1$)
 337 and selection occurred, potentially resulting in genetic evolution across generations.

338 Several variants of scenario B were also considered as follows:

- 339 – Scenario **C (“Evolution without mortality”)**, in which F_{critBB} was variable and
 340 heritable ($h^2=1$) and selection occurred only through differential reproduction without
 341 mortality.
- 342 – Scenario **D (“Evolution without differential reproduction”)**, in which F_{critBB} was
 343 variable and heritable ($h^2=1$) and selection occurred only through differential mortality
 344 without differential reproduction among individuals.

- 345 – Scenario **E** (“**Evolution, mortality driven by low level of cumulated carbon**
 346 **reserve**”), in which mortality only occurred when the carbon reserve at the end of the
 347 year (CumCR) fell below a critical value (Type I mortality, Table 1).
- 348 – Scenario **F** (“**Evolution, mortality driven by low level of carbon reserve at**
 349 **budburst**”), in which mortality only occurred when the carbon reserve before
 350 budburst (bbCR) fell below a critical value (Type II mortality, Table 1).
- 351 – Scenario **G** (“**Evolution, reduced heritability**”), in which the heritability of F_{critBB}
 352 was set to $h^2=0.6$.
- 353 – Scenario **H** (“**Evolution with frost effect on LAI**”), in which every late frost reduced
 354 the LAI (Ha) by 10% or (Hb) by 20% per degree below the critical minimal
 355 temperature.

356 For each scenario, we ran 21 repetitions with different random initial conditions. Among the
 357 repetitions, only the spatial locations and the 500 initial founder genotypes changed, whereas
 358 the allelic effects at each QTL were the same (Table 1). The average genetic value for F_{critBB}
 359 in the initial founder population was always $\mu_{FcritBB}=190$. The same allelic effects were used
 360 for all replicate runs of the simulation.

361 *Simulation result analyses*

362 The continuous population ranging between 700 and 1700 m in elevation was split into five
 363 discrete adjacent populations, namely, Alt1 (700-900 m), Alt2 (900-1100 m), Alt3 (1100-
 364 1300 m), Alt4 (1300-1500 m) and Alt 5 (1500-1700 m). Output variable distributions were
 365 obtained for each tree from the 30-year sequence (from ages 40 to 70).

366 We computed the change of F_{critBB} and TBB between generations G0 and G5 (Cb) population
 367 per population. As F_{critBB} was constant across the lifetime for a given tree, the change of
 368 F_{critBB} was estimated as follows:

$$Cb_{F_{critBB}} = \frac{1}{n_{rep} n_{rep}} \sum (\mu_{Y40G5} - \mu_{Y40G0}) \quad (13)$$

where n_{rep} is the number of repetitions (here $n_{rep}=5$) and μ_{YnGx} is the average F_{critBB} -value at year n of generation X within the population under consideration (Y40 corresponded to the first year of the adult life stage).

By contrast, TBB varied among the different climatic years (2002 to 2006). The change of TBB was estimated as follows:

$$Cb_{TBB} = \frac{1}{n_{rep} n_{rep}} \sum \left(\frac{1}{n_{climYear}} \sum_{y=0}^4 (\mu_{Y40+y,G5} - \mu_{Y40+y,G0}) \right) \quad (11)$$

where $n_{climYear}=5$, and $y=0$ for year 2002 up to $y=4$ for year 2006.

To measure the strength of within-generation selection, we also computed the change within each generation Gx as follows for F_{critBB} :

$$Cw_{F_{critBB}}(Gx) = \frac{1}{n_{rep} n_{rep}} \sum (\mu_{Y70Gx} - \mu_{Y40Gx}) \quad (14)$$

Note that both Cw and Cb are classically used in quantitative genetics; Cw is also referred to as the selection differential (the difference of the mean trait value in a population before and after an episode of selection), and Cb measures the response to selection (the difference between the population distribution before selection and the distribution of the trait in the next generation). Cw - and Cb -values were compared between populations and scenarios using simple linear models with interaction between populations and scenarios (online Appendix 4). All analyses were performed with R (RDevelopmentCoreTeam, 2010).

Results

Because population Alt1 collapsed in almost all simulations (because of strong mortality below 800 m), it was excluded from the population-level results.

390 *Plastic response to the climatic gradient (scenario A)*

391 Only surviving trees were used for this analysis. Across all climatic years and all adult life
392 stages the length of growing season decreased on average from 210 to 160 days (Fig. 3A), and
393 the water stress index (WSI) decreased by 33% between 1000 and 1700 m (Fig. 3B). As a
394 consequence of these two limiting factors, the highest photosynthesis level ($GPP=1216 \text{ g}_C\cdot\text{m}^{-2}$)
395 occurred at 1078 m (Fig. 3C), and was almost as high from ~1050 to ~1300 m. However, as
396 respiratory costs also strongly decreased above 1200 m (Fig. 3D), the highest ring increment
397 and seed production values were found at 1258 m (Fig. 3E) and 1204 m (Fig. 3F),
398 respectively. At elevations >1400 m, the ring width decrease was steeper than the seed
399 production decrease. The minimal value of carbon reserves at the end of the year occurred
400 between 1160 and 1420 m, and the greatest difference between carbon reserves and carbon
401 demand during budburst was found below 1000 m (Fig. S1). Mortality was higher, on
402 average, at low/intermediate elevations (Table S3).

403 The physiological response to the elevational gradient varied significantly among climatic
404 years. For instance, ring widths were large regardless of elevation in 2002, but in 2003, they
405 increased continuously with the elevation, and in 2004, 2005 and 2006, they reached a
406 maximum at 1000 m, 1100 and 1200 m, respectively (Fig. S2A). This variability among years
407 was also observed for seed production and the level of carbon reserves at the end of the year
408 (Fig. S2B).

409 *Adaptive response of F_{critBB} to the climatic gradient*

410 To investigate the effect of genetic adaptation along the gradient, we compared scenario B
411 (adaptive evolution with $h^2_{F_{critBB}}=1$) with scenario A (neutral with $h^2_{F_{critBB}}=0$). First, we
412 observed significant differences among scenarios and populations for the patterns of changes
413 in F_{critBB} between generations G0 and G5 (denoted $Cb_{F_{critBB}}$), which measures the response to
414 selection (Table 2, Fig. 4A-B, online Appendix 4). In scenario A, $Cb_{F_{critBB}}$ was low ($< 1^\circ\text{C}$) in

415 all populations. In scenario B, absolute $Cb_{F_{critBB}}$ -values were significantly higher than in
416 scenario A in populations Alt2 to Alt 4 (online Appendix 4). Populations Alt3 and Alt4
417 evolved toward lower F_{critBB} values (on average, $Cb_{F_{critBB}}=-4.72^{\circ}\text{C}$ in Alt3 and -2.85°C in
418 Alt4, Fig. 4), while population Alt2 evolved toward a higher F_{critBB} (on average,
419 $Cb_{F_{critBB}}=+1.18^{\circ}\text{C}$).

420 Secondly, we investigated patterns of change in F_{critBB} within each generation (Cw), as a
421 measure of the strength of selection (Table 2, Fig.5). Patterns of $Cw_{F_{critBB}}$ were similar among
422 scenarios A and B at generation G0, with negative $Cw_{F_{critBB}}$ -values within populations Alt3 to
423 Alt5 ($Cw_{F_{critBB}}=-3.61^{\circ}\text{C}$, in Alt3, scenario B), and a positive $Cw_{F_{critBB}}$ -value in population
424 Alt2 ($Cw_{F_{critBB}}=+1.57^{\circ}\text{C}$, scenario B). Differences in absolute $Cw_{F_{critBB}}$ values indicate that
425 selection was two-fold more intense in population Alt3 than Alt2 or Alt4, and it was weak in
426 population Alt5. These variations in selection direction and strength were consistent with the
427 variations of F_{critBB} observed among generations (Cb) in scenario B. Finally, patterns of
428 $Cw_{F_{critBB}}$ at generation G5 differed among scenarios A and B. While $Cw_{F_{critBB}}$ -values
429 remained similar across generation in scenario A, $Cw_{F_{critBB}}$ -values decreased across
430 generations in scenario B as a consequence of selection and recombination (Fig. 5). The
431 phenotypic variances for F_{critBB} within each population were also slightly lower in scenario B
432 than in scenario A at generation G5, in particular in Alt3 (Table 2).

433 *Deciphering the mechanisms driving microevolution of F_{critBB}*

434 We investigated the effects of differential reproduction and differential mortality on
435 evolutionary dynamics by comparing scenarios A, B, C and D. Scenario without mortality
436 (scenario C) led to weak changes in F_{critBB} from G0 to G5 (Fig. 4C), but overall the pattern of
437 $Cb_{F_{critBB}}$ did not significantly differ from scenario A (online Appendix 4), indicating that the
438 absence of mortality prevented genetic adaptation. In contrast, scenario without differential
439 reproduction (scenario D) resulted in a change of F_{critBB} from G0 to G5 that was as important

440 as it was in scenario B (Fig. 4D), indicating that differential reproduction between trees
441 played a minor role in simulated patterns of adaptation.

442 We also investigated the variations of $C_{b_{F_{critBB}}}$ in Scenario E, where mortality was driven by
443 low levels of accumulated carbon reserves (Type I mortality) and scenario F where mortality
444 was driven by low carbon reserve levels at budburst (Type II mortality). In scenario E,
445 populations Alt3 and Alt4 still evolved significantly toward a lower F_{critBB} as compared to
446 scenario A, but the population Alt2 did not evolve toward higher F_{critBB} (Fig. 4E, online
447 Appendix 4). This trend was caused by the absence of Type I mortality at low elevations
448 (Table S3). In scenario F, population Alt2 still evolved towards a higher F_{critBB} but
449 populations Alt3 and Alt4 did not evolve toward a lower F_{critBB} (Fig. 4F). This result was due
450 to the absence of Type II mortality in these populations (Table S3). The patterns of $C_{W_{F_{critBB}}}$
451 values within populations in scenarios F and G were consistent with these C_b patterns (Fig.
452 S3).

453 Mortality not only drove evolution in F_{critBB} but also affected the elevational range of the
454 population. In scenarios A, and D, the range of the whole population (as measured by the
455 average elevation) shifted by on average +202m and +168 m respectively between
456 generations G0 and G5 (with minimal elevation ~800 m), which could be due to higher
457 mortality/lower reproduction at low elevation. By contrast, in scenario C and E, the
458 elevational shift of the whole population was reduced (+37 m and +16m respectively), and the
459 minimal elevation at G5 was ~720 m.

460 *Effect of heritability on genetic adaptation*

461 The heritability-level effects of F_{critBB} on the micro-evolutionary patterns of F_{critBB} were
462 analyzed by comparing scenario B ($h^2=1$) to scenario G ($h^2=0.6$). The divergence among
463 populations that evolved positive (Alt2) versus negative (Alt3 and Alt4) values for F_{critBB} was

464 reduced when heritability was lower (Fig. 4). However, the response to selection remained
465 important in populations Alt3 and Alt4 ($Cb_{FcritBB} = -3.79^{\circ}\text{C}$ and -2.07°C , respectively).

466 *Impact of frost on evolutionary dynamics*

467 We investigated the effects of frost by using scenarios including a moderate (scenario Ha) or
468 strong frost effect (scenario Hb) on the leaf area index (LAI). The patterns of microevolution
469 markedly changed when compared to scenario B (Fig. 4). Population Alt2 no longer evolved
470 toward higher values for F_{critBB} , and population 3 no longer evolved toward lower values of
471 F_{critBB} . Only population Alt4 evolved toward a lower F_{critBB} value ($Cb_{FcritBB} = -4.96^{\circ}\text{C}$ and -
472 3.55°C for scenarios Ha and Hb, respectively). The Cw patterns for F_{critBB} also consistently
473 indicated that selection was strongest in population Alt4 (Fig. S3). Finally, frost effect
474 promoted a reduced elevational shift of the whole population for scenarios Ha and Hb (+75.1
475 m and +27.1 m, respectively) in comparison to scenario B (+167 m), which resulted from less
476 severe mortality at lower elevations (Table S3).

477 **Discussion**

478 *Effects of plasticity and microevolution on TBB variation*

479 Trees are long-lived species, and they experience a high variability in environmental
480 conditions during their lives because of differences between the juvenile and adult stages and
481 variations among climatic years. Accordingly, trees are expected to display a high plasticity
482 for a wide range of functional traits, including TBB. In our baseline neutral scenario (A), the
483 TBB varied by 12.2 days, on average, between the two extreme climatic years (and therefore
484 $7.6 \text{ days}\cdot\text{degree}^{-1}$) and by 35.2 days between the two extreme elevations (and therefore 5.4
485 $\text{days}\cdot\text{degree}^{-1}$). This plastic variation was within the TBB range reported for *F. sylvatica* by
486 Vitasse et al. (2011), who found a range of TBB from 4.9 to $5.8 \text{ days}\cdot\text{degree}^{-1}$ across an
487 elevational gradient from 131 and 1533 m in the Pyrenees. However, a lower plasticity was

488 found in previous studies (between 2 days.degree⁻¹ and 2.5 days.degree⁻¹ (Kramer *et al.*, 2008;
489 Menzel *et al.*, 2001).

490 In comparison to the plasticity, the TBB variation resulting from microevolution was small.
491 Between the two most genetically differentiated populations (e.g., between populations Alt2
492 and Alt3 at generation G5) in the baseline scenario of adaptive evolution (B), the difference of
493 5.9°C in the temperature sum required for budburst (F_{critBB} , the genetic component of TBB)
494 corresponded to an average of two days for TBB (Fig S4). These small variations are
495 consistent with previous experimental studies; Vitasse *et al.* (2009b) found that a phenological
496 model with constant parameters is able to reproduce TBB for different populations,
497 suggesting that plasticity hides local adaptation. Using a common garden experiment, Vitasse
498 *et al.* (2009b) also reported that the genetic difference in TBB between populations
499 originating from different elevations was almost four days, which is above our estimation of
500 two days due to a wider elevational range. However, it is also likely that more differentiation
501 would be found when simulating responses over more than 5 generations.

502

503 *Non-monotonic elevation effects on the TBB genetic optimum*

504 Although they were weaker than phenotypic differentiation, significant patterns of genetic
505 differentiation for TBB across elevations were nonetheless obtained in only five generations.
506 In scenario B, one population (Alt2) evolved toward delayed budburst (F_{critBB} increase of
507 $=+1.18^{\circ}\text{C}$), whereas populations Alt3 and Alt4 evolved toward earlier budburst (F_{critBB}
508 decrease of -2.85° to -4.72°C). The resulting pattern of F_{critBB} variation across elevations was
509 thus non-monotonic. This result occurred because the mortality in population Alt2 was
510 triggered by a lack of sufficient reserves before budburst to produce new leaves (Type II
511 mortality, scenario E), and in populations Alt3 to Alt5, mortality was triggered by low
512 reserves during the winter (Type I mortality, scenario F). The variability across elevations in

513 mortality-triggering factors resulted from the non-linear variability of the underlying eco-
514 physiological processes, which makes the trees located at different elevations pass different
515 thresholds to mortality during different years. Type I mortality occurred mainly during 2004
516 for trees from populations Alt3 to Alt5, and Type II mortality occurred mainly during 2003
517 for trees located below 1100 m (i.e., populations Alt2 and Alt1). In population Alt2, fewer
518 trees displayed low reserves during winter in comparison to trees at higher elevations, because
519 of longer growth period. However, these trees also displayed a higher leaf area index (LAI)
520 and biomass, which increased the respiratory and construction costs before budburst and
521 made them more vulnerable to Type II mortality.

522 When frost damage was considered (scenario Ha and Hb), other non-monotonic effects were
523 observed. As only trees that initiated budburst could suffer from late frost, frost damage did
524 not occur at the upper elevations (e.g., population Alt4) because delayed budburst protected
525 them from late frosts. The first mechanistic consequence is that frost did not linearly affect the
526 trees across the elevational gradient. Second, reduced LAI from frost damage can either
527 increase or decrease the risk of mortality depending on its absolute effect for the reserve level.
528 The risk of Type II mortality is expected to increase with frost damage because a reduced LAI
529 decreases the carbon assimilation rate. However, a moderate frost in the model can also
530 reduce Type I mortality because reduced LAI can decrease the carbon reserve required during
531 budburst and the water loss during the following summer. This phenomenon explains why,
532 when frost damage was considered, population Alt2 became less sensitive to carbon demand
533 before budburst and did not evolve toward a later budburst as in the baseline scenario B.

534 This study sheds light on the mechanisms that underlie genetic and phenotypic patterns of
535 TBB variation. Considering the number of underlying mechanisms involved in TBB and their
536 patterns of environmental variation, this study suggests that non-monotonic genetic patterns
537 of TBB variation should be the rule rather than the exception. Other factors not considered

538 here (for instance, assortative mating induced by variations in reproductive phenology across
539 elevation) should be further studied (Soularue & Kremer, 2012).

540 *Understanding the mechanisms underlying climate adaptation*

541 This study was based on a new mechanistic model coupling physiology, population dynamics
542 and quantitative genetics to simulate the short-term evolution of functional traits. Because
543 PDG explicitly accounts for climate effects on the water and carbon exchanges of individual
544 trees as a selective pressure, it provides a useful complement to existing evolutionary models
545 of tree population life history traits (Kuparinen *et al.*, 2010; Le Corre & Kremer, 2003). More
546 precisely, in PDG as in these other models, individual fitness is the parameter driving the
547 process of adaptation. However, the primary originality of PDG is that individual fitness is an
548 output, which is calculated as the lifetime reproductive success resulting from a combination
549 of functional traits and the environmental context. This was also used (Kramer *et al.*, 2008) to
550 investigate the temporal patterns of microevolution in a single population. We extended this
551 approach here, and we showed how such a mechanistic model can be used to investigate the
552 type and strength of selection mediated by the climate through the estimation of the selection
553 differential (by using C_w , the difference in the population before and after an episode of
554 selection).

555 In PDG, selection occurred both through differential mortality and reproduction of individual
556 trees within each generation. Mortality was found to be the main driver of evolutionary
557 dynamics, with different types of mortality promoting different patterns of adaptation across
558 elevations. Predicting tree mortality is a key and complex issue in tree physiology and
559 ecology because many mechanisms are involved and interact (carbon starvation, cavitation
560 and pathogens, (McDowell *et al.*, 2008). We chose to model tree mortality according to the
561 carbon starvation hypothesis alone, in which a tree dies when carbon reserves are too low to
562 allow the set-up of new leaves in the spring (second threshold, Type II mortality) or to ensure

563 tree functioning during the winter (first threshold, Type I mortality). We excluded two other
564 mechanisms because (1) no major pathogens were observed in our site for *F. sylvatica* and (2)
565 in Ventoux the minimal hydraulic potential (-2 Mpa) is above the critical pressure causing a
566 50% loss of conductance (-2.4 Mpa , Herbette *et al.*, 2010).

567 In contrast, differential reproduction among individuals was found to have a minor role as a
568 driver of evolutionary dynamics. To our knowledge, few models relate reproduction to tree
569 carbon cycles (Génard *et al.*, 2008). Our main hypothesis here was that seed production
570 increases with carbohydrate reserves. This idea is consistent with the higher seed production
571 observed for dominant trees (Davi, pers. obs.) and for years after good climatic years. It is
572 also consistent with the resource supply hypothesis, in which fruit production, especially
573 during mast years, occurs when carbohydrate reserves are sufficient (Yamauchi, 1996).

574 In addition to selection, the outcome of adaptation is also determined by the level of genetic
575 variation available for selection, which depends on the heritability of the trait under selection,
576 and on genetic architecture (in particular, the number of QTLs determining the trait's genetic
577 variation). We showed that levels of heritability for the timing of budburst such as those
578 measured for *F. sylvatica* ($h^2=0.6$, Kramer *et al.*, 2008) lead to significant patterns of genetic
579 differentiation for the TBB across elevations. It was out of the scope of this study to
580 investigate genetic architecture effects in detail. Therefore, we chose a simple additive
581 quantitative genetic model with ten independent QTLs for TBB, as in previous studies
582 (Kuparinen *et al.*, 2010; Le Corre & Kremer, 2003). However, further investigations into the
583 effects of the quantitative genetic model are needed (Le Corre & Kremer, 2012).

584 ***Main shortcomings of the mechanistic Physio-Demo-Genetic model***

585 Admittedly, full PDG evaluation requires the parameterization and evaluation of complex
586 mechanisms of tree physiology, demography and selection that was beyond the scope of the
587 present paper. Among the most important shortcomings of this study, we repeatedly re-used a

588 short (five-year) climatic period that is clearly unrealistic and potentially biases the estimates
589 of survival between generations. Moreover this period included specific climatic years, which
590 can have major influence on results. For instance, 2004 was an exceptional drought year that
591 has led to low growth rates of beeches (Cailleret & Davi, 2011). Second, PDG does not
592 include competition between adult trees, which is a process that is potentially more important
593 for tree growth and survival than climate. However, not accounting for competition in
594 studying microevolution driven by TBB is reasonable because TBB is related primarily to
595 temperature and only secondarily to competition. Indeed, we previously showed that
596 dominant trees exhibited an earlier TBB, but this effect is small in comparison with the
597 elevation and year effects (Davi et al., 2011). Third, we used non-overlapping generations,
598 which make individual level comparisons with forest inventory data and tree ring increment
599 measurements difficult. Fourth, dormancy was not taken into account in modeling *F. sylvatica*
600 budburst. Fifth, a real sensitivity analysis on the entire model (as done for the eco-
601 physiological component of PDG in Dufrière et al., 2005) will be needed to strengthen some
602 of our conclusions and to draw a more accurate picture of what process control genetic
603 adaptation of budburst.

604 Nevertheless, valid conclusions could be drawn using the current version of PDG. This
605 success is possible mainly because the physiological module of PDG (CASTANEA), which
606 models the climate effect on tree functioning, has already been thoroughly validated for
607 European beech in several previous studies (e.g., Dufrière *et al.*, 2005). PDG simulated the
608 maximum tree ring width for elevations between 1100 and 1420 m, which also corresponds to
609 the maximum ring width observed in the field (Cailleret & Davi, 2011).

610 Conclusions

611 We described here a new modeling tool (PDG) to assess the potential mechanisms of local
612 adaptation for trees under changing environmental conditions. The primary originalities of the

613 PDG model is that it combines physiology, demography and genetics, and that fitness is a
614 dynamic output of the model. Such complex models are useful tools for predicting the
615 evolution of non-equilibrium forest populations under CC, under which many tipping points
616 and non-linear effects may be involved. PDG model requires a large amount of data to be
617 parameterized and tested, and results must be cautiously interpreted. Demographic processes
618 such as mortality and reproduction should be further studied, and other processes such as
619 competition and regeneration have to be included in this general framework. Nevertheless, the
620 following TWO important conclusions emerge from our present study: (i) genetic evolution of
621 tree populations can occur in a few generations (<5), and (ii) patterns of genetic
622 differentiation across space (and across elevations here) can be non-monotonic.

623 Data Archiving Statement

624 The raw simulation data underlying the main results of the study will be archived.

625 References

- 626 Alberto, F.J., Aitken, S.N., Alía, R., González-Martinez, S.C., Hänninen, H., Kremer, A.,
627 Lefèvre, F.o., Lenormand, T., Yeaman, S., Whetten, R., & Savolainen, O. (2013)
628 Potential for evolutionary responses to climate change “evidence from tree
629 populations. *Global Change Biology*, **19**, 1645-1661.
- 630 Bontemps, A. (2012) Potentiel évolutif d'une population de hêtre commun sur le Mont
631 Ventoux, University Paul Cézanne, Aix-Marseille III, Aix en Provence.
- 632 Bontemps, A., Klein, E.K., & Oddou-Muratorio, S. (2013) Shift of spatial patterns during
633 early recruitment in *Fagus sylvatica*: evidence from seed dispersal estimates based on
634 genotypic data. *Forest Ecology and Management*, **305**, 67-76.
- 635 Bost, B., de Vienne, D., Hospital, F., Moreau, L., & Dillman, C. (2001) Genetic and
636 nongenetic bases for the L-shaped distribution of quantitative trait loci effects.
637 *Genetics*, **157**, 1773-1787.

- 638 Cailleret, M. & Davi, H. (2011) Effects of climate on diameter growth of co-occurring *Fagus*
639 *sylvatica* and *Abies alba* along an altitudinal gradient. *Trees*, **25**, 265-276 LA -
640 English.
- 641 Chevin, L.-M., Collins, S., & Lefèvre, F. (2013) Phenotypic plasticity and evolutionary
642 demographic responses to climate change: taking theory out to the field. *Functional*
643 *Ecology*, **27**, 967-979.
- 644 Davi, H., Barbaroux, C., Francois, C., & Dufrêne, E. (2009) The fundamental role of reserves
645 and hydraulic constraints in predicting LAI and carbon allocation in forests.
646 *Agricultural and Forest Meteorology*, **149**, 349-361.
- 647 Davi, H., Baret, F., Huc, R., & Dufrêne, E. (2008) Effect of thinning on LAI variance in
648 heterogeneous forests. *Forest Ecology and Management*, **256**, 890-899.
- 649 Davi, H., Dufrêne, E., Granier, A., Le Dantec, V., Barbaroux, C., François, C., & Bréda, N.
650 (2005) Modelling carbon and water cycles in a beech forest: Part II.: Validation of the
651 main processes from organ to stand scale. *Ecological Modelling*, **185**, 387-405.
- 652 Davi, H., Gillmann, M., Ibanez, T., Cailleret, M., Bontemps, A., Fady, B., & Lefèvre, F.
653 (2011) Diversity of leaf unfolding dynamics among tree species: New insights from a
654 study along an altitudinal gradient. *Agricultural and Forest Meteorology*, **151**, 1504-
655 1513.
- 656 Dittmar, C. & Elling, W. (2006) Phenological phases of common beech (*Fagus sylvatica* L.)
657 and their dependence on region and altitude in Southern Germany. *European Journal*
658 *of Forest Research*, **125**, 181-188.
- 659 Dufour-Kowalski, S., Courbaud, B., Dreyfus, P., Meredieu, C., & de Coligny, F. (2012)
660 Capsis: an open software framework and community for forest growth modelling.
661 *Annals of Forest Science*, **69**, 221-233.

- 662 Dufrière, E., Davi, H., Francois, C., le Maire, G., Le Dantec, V., & Granier, A. (2005)
- 663 Modelling carbon and water cycles in a beech forest Part I: Model description and
- 664 uncertainty analysis on modelled NEE. *Ecological Modelling*, **185**, 407-436.
- 665 Génard, M., Dauzat, J., Franck, N., Lescourret, F., Moitrier, N., Vaast, P., & Vercambre, G.
- 666 (2008) Carbon allocation in fruit trees: from theory to modelling. *Trees*, **22**, 269-282
- 667 LA - English.
- 668 Ghalambor, C.K., Mckay, J.K., Carroll, S.P., & Reznick, D.N. (2007) Adaptive versus non-
- 669 adaptive phenotypic plasticity and the potential for contemporary adaptation in new
- 670 environments. *Functional Ecology*, **21**, 394-407.
- 671 Gomory, D. & Paule, L. (2011) Trade-off between height growth and spring flushing in
- 672 common beech (*Fagus sylvatica* L.). *Annals of Forest Science*, **68**, 975-984.
- 673 Han, Q.M., Kabeya, D., & Hoch, G. (2011) Leaf traits, shoot growth and seed production in
- 674 mature *Fagus sylvatica* trees after 8 years of CO₂ enrichment. *Annals of Botany*, **107**,
- 675 1405-1411.
- 676 Hansen, M.M., Olivieri, I., Waller, D.M., Nielsen, E.E., & Group, T.G.W. (2012) Monitoring
- 677 adaptive genetic responses to environmental change. *Molecular Ecology*, no.
- 678 Herbette, S., Wortemann, R., Awad, H., Huc, R., Cochard, H., & Barigah, T.S. (2010)
- 679 Insights into xylem vulnerability to cavitation in *Fagus sylvatica* L.: phenotypic and
- 680 environmental sources of variability. *Tree Physiology*, **30**, 1448-1455.
- 681 Kramer, K., Buiteveld, J., Forstreuter, M., Geburek, T., Leonardi, S., Menozzi, P., Povillon,
- 682 F., Schelhaas, M.J., Teissier du Cros, E., Vendramin, G.G., & van der Werf, D.C.
- 683 (2008) Bridging the gap between ecophysiological and genetic knowledge to assess
- 684 the adaptive potential of European beech. *Ecological Modelling*, **216**, 333-353.
- 685 Kremer, A. & Le Corre, V. (2011) Decoupling of differentiation between traits and their
- 686 underlying genes in response to divergent selection. *Heredity*, **108**, 375-385.

- 687 Kremer, A., Ronce, O., Robledo-Arnuncio, J.J., Guillaume, F., Bohrer, G., Nathan, R., Bridle,
688 J.R., Gomulkiewicz, R., Klein, E.K., Ritland, K., Kuparinen, A., Gerber, S., &
689 Schueler, S. (2012) Long-distance gene flow and adaptation of forest trees to rapid
690 climate change. *Ecology Letters*, **15**, 378-392.
- 691 Kuparinen, A., Savolainen, O., & Schurr, F.M. (2010) Increased mortality can promote
692 evolutionary adaptation of forest trees to climate change. *Forest Ecology and*
693 *Management*, **259**, 1003-1008.
- 694 Labonne, J. & Hendry, A.P. (2010) Natural and sexual selection can giveth and taketh away
695 reproductive barriers: models of population divergence in guppies. *The American*
696 *Naturalist*.
- 697 Le Corre, V. & Kremer, A. (2003) Genetic Variability at Neutral Markers, Quantitative Trait
698 Loci and Trait in a Subdivided Population Under Selection. *Genetics*, **164**, 1205-1219.
- 699 Le Corre, V. & Kremer, A. (2012) The genetic differentiation at quantitative trait loci under
700 local adaptation. *Molecular Ecology*, **21**, 1548-1566.
- 701 McDowell, N., Pockman, W.T., Allen, C.D., Breshears, D.D., Cobb, N., Kolb, T., Plaut, J.,
702 Sperry, J., West, A., Williams, D.G., & Yezzer, E.A. (2008) Mechanisms of plant
703 survival and mortality during drought: why do some plants survive while others
704 succumb to drought? *New Phytologist*, **178**, 719-739.
- 705 Menzel, A., Estrella, N., & Fabian, P. (2001) Spatial and temporal variability of the
706 phenological seasons in Germany from 1951 to 1996. *Global Change Biology*, **7**, 657-
707 666.
- 708 Nicotra, A.B., Atkin, O.K., Bonser, S.P., Davidson, A.M., Finnegan, E.J., Mathesius, U.,
709 Poot, P., Purugganan, M.D., Richards, C.L., Valladares, F., & van Kleunen, M. (2010)
710 Plant phenotypic plasticity in a changing climate. *Trends in Plant Science*, **15**, 684-
711 692.

- 712 Oddou-Muratorio, S., Bontemps, A., Klein, E.K., Chybicki, I.J., Vendramin, G.G., &
713 Suyama, Y. (2010) Comparison of direct and indirect genetic methods for estimating
714 seed and pollen dispersal in *Fagus sylvatica* and *Fagus crenata*. *Forest Ecology and*
715 *Management*, **259**, 2151–2159.
- 716 Polechová, J., Barton, N., & Marion, G. (2009) Species' Range: Adaptation in Space and
717 Time. *American Naturalist*, **174**, E186-E204.
- 718 Porté, A., Huard, F., & Dreyfus, P. (2004) Microclimate beneath pine plantation, semi-mature
719 pine plantation and mixed broadleaved-pine forest. *Agricultural and Forest*
720 *Meteorology*, **126**, 175-182.
- 721 RDevelopmentCoreTeam (2010) R: A language and environment for statistical computing
722 (ed R.F.f.S. Computing.), Vienna, Austria.
- 723 Rehfeldt, G.E., Tchebakova, N.M., Parfenova, Y.I., Wykoff, W.R., Kuzmina, N.A., &
724 Milyutin, L.I. (2002) Intraspecific responses to climate in *Pinus sylvestris*. *Global*
725 *Change Biology*, **8**, 912-929.
- 726 Richardson, A.D., Bailey, A.S., Denny, E.G., Martin, C.W., & O'Keefe, J. (2006) Phenology
727 of a northern hardwood forest canopy. *Global Change Biology*, **12**, 1174-1188.
- 728 Savolainen, O., Pyhajarvi, T., & Knurr, T. (2007) Gene Flow and Local Adaptation in Trees.
729 *Annual Review of Ecology, Evolution, and Systematics*, **38**, 595-619.
- 730 Soularue, J.-P. & Kremer, A. (2012) Assortative mating and gene flow generate clinal
731 phenological variation in trees. *BMC Evolutionary Biology*, **12**, 79.
- 732 Vitasse, Y., Delzon, S., Bresson, C.C., Michalet, R., & Kremer, A. (2009a) Altitudinal
733 differentiation in growth and phenology among populations of temperate-zone tree
734 species growing in a common garden. *Canadian Journal of Forest Research*, **39**,
735 1259-1269.

- 736 Vitasse, Y., Delzon, S., Dufrêne, E., Pontailier, J.-Y., Louvet, J.-M., Kremer, A., & Michalet,
737 R. (2009b) Leaf phenology sensitivity to temperature in European trees: Do within-
738 species populations exhibit similar responses? *Agricultural and Forest Meteorology*,
739 **149**, 735-744.
- 740 Vitasse, Y., Francois, C., Delpierre, N., Dufrene, E., Kremer, A., Chuine, I., & Delzon, S.
741 (2011) Assessing the effects of climate change on the phenology of European
742 temperate trees. *Agricultural and Forest Meteorology*, **151**, 969-980.
- 743 von Wuehlisch, G., von Krusche, D., & Muhs, H.J. (1995) Variation in temperature sum
744 requirement for flushing of beech provenances. *Silva Genetica*, **44**, 5-6.
- 745 Yamauchi, A.D. (1996) Theory of Mast Reproduction in Plants: Storage-Size Dependent
746 Strategy. *Evolution*, **50**, 1795-1807.
- 747
- 748
- 749

750 **Table 1:** List of PDG parameters.

751

Parameter	Acronym	Value	Unit	Sources
Physical/physiological CASTANEA module				
Canopy clumping		0.56	-	Davi et al. (2008)
Nitrogen content		2.2	%	Bontemps (2012)
Leaf mass per area		93	g _{DM} m ⁻²	Bontemps (2012)
Relationship between maximal rate of carboxylation and nitrogen		26.04	μmol CO ₂ gN ⁻¹ s ⁻¹	Ducrey & Huc (pers. comm.)
Date of rest onset for budburst		78	Days	Davi (unpublished data)
Average critical value of forcing state	μF _{critBB}	190	°C	this study
Base temperature for forcing budburst		0	°C	Fixed
Ratio between fine root and leaf biomass		1	-	Fixed
Soil extractable water	SEW	60	Mm	Nourtier (2011)
Threshold value for frost effect on LAI	T _{minEffect}	0	°C	Fixed
Demographic module				
Critical threshold of carbon reserves at the end of the year for reproduction	sB _{res}	100	gC m _{soil} ⁻²	Fixed
Critical threshold of carbon reserves at the end of the year	CumCR	45	gC m _{soil} ⁻²	Fixed
Maximal difference between carbon needs and carbon reserves before budburst	bbCR	160	gC m _{soil} ⁻²	Fixed
Rate of seed production	R _{SP}	0.05	-	Fixed
Cost to produce one seed	C	0.45	gC	Han et al., 2011
Rate of empty seeds	r _{ES}	0.33	-	Oddou-Muratorio, pers. obs.
Rate of seed germination	r _{SG}	0.485	-	Oddou-Muratorio, pers. obs.
Rate of seed survival	r _{SS}	0.15	-	
Average distance of seed dispersal	Δs	18.13	m	Bontemps et al. (2013)
Shape of the seed dispersal kernel	b _S	0.31		Bontemps <i>et al.</i> (2013)
Average distance of pollen dispersal	δ _p	37.9	m	Bontemps et al. (2013)
Shape of the pollen dispersal kernel	b _p	0.97		Bontemps et al. (2013)
Parameter relating tree diameter and male fertility	γ _m	0.82	-	Bontemps et al. (2013)
Rate of selfing	S	0.025		Bontemps et al. (2013)

Mean height of newly recruited tree	μ_H	9	m	Dreyfus (pers. comm.)
Standard deviation of newly recruited tree height	sd_H	0.34	m	Dreyfus (pers. comm.)
Mean DBH of newly recruited tree	μ_{DBH}	13.8	cm	Dreyfus (pers. comm.)
Standard deviation of newly recruited tree DBH	sd_{DBH}	0.9	cm	Dreyfus (pers. comm.)

752

753

754

755

Table 2: Simulated patterns of evolution for the temperature sum required for budburst (F_{critBB}). For each population, the changes in F_{critBB} within generation G0 (C_w) measures the intensity of selection while the change between generations G0 and G5 (C_b) measures the response to selection. The phenotypic variance for F_{critBB} (V_P) was computed at the last year of generation G5; in scenarios with $h^2=1$ (B to F; Ha and Hb), V_P is also the additive variance V_A . In scenario A, $V_A=0$; in scenario G, $V_P = V_A + V_E$. Population Alt1 is not shown because of low population size.

Population	Alt2			Alt3			Alt4			Alt5		
	C_b	C_w	V_P									
<												
A- Neutral	-0.42	1.32	21.68	0.48	-4.28	18.11	-0.08	-1.06	21.13	0.00	-0.15	21.37
B- Adaptive evolution	1.18	1.57	21.21	-4.72	-3.61	13.60	-2.85	-1.11	20.18	-1.06	-0.21	19.64
C- Evolution without mortality	0.00	0.00	21.15	-0.24	0.00	19.43	-0.52	0.00	20.51	-0.31	0.00	21.10
D- Evolution without differential reproduction	1.33	1.36	21.68	-4.76	-3.47	14.55	-2.69	-0.81	19.40	-0.88	-0.15	20.41
E- Evolution, Type I mortality	-0.23	0.00	19.64	-4.93	-3.72	14.81	-2.63	-1.06	19.03	-0.94	-0.18	20.39
F- Evolution, Type II mortality	0.55	0.98	20.34	-0.03	-0.01	19.81	0.03	0.00	20.50	0.06	0.00	19.98
G- Evolution, reduced heritability	0.60	1.88	33.72	-3.79	-6.09	24.84	-2.07	-1.60	32.31	-0.90	-0.35	31.49
Ha- Evolution, moderate effect of frost	-1.21	-0.40	18.37	-0.41	-0.02	20.30	-3.71	-2.07	17.43	-0.93	-0.30	18.37
Hb- Evolution, strong effect of frost	-1.15	-0.39	18.61	-0.21	0.03	19.42	-4.01	-3.15	18.21	-1.17	-0.33	19.57

1 List of Figures

2 **Figure 1:** Observed budburst in Mont Ventoux versus simulated budburst using an average
3 value of 190°C for the temperature sum required for budburst (F_{critBB}).

4 **Figure 2:** Spatial population dynamics over five generations (from G0 to G5) under “adaptive
5 evolution” scenario (B) along the elevational gradient.

6 **Figure 3:** Elevational plastic variation of (A) length of growing season (LGS), (B) water
7 stress index (WSI), (C) gross primary production (GPP), (D) plant respiration (PR), (E) ring
8 width (RW) and (F) seed production (SP). Each point corresponds to the average value across
9 climatic years of the variable of interest for surviving trees (Scenario B).

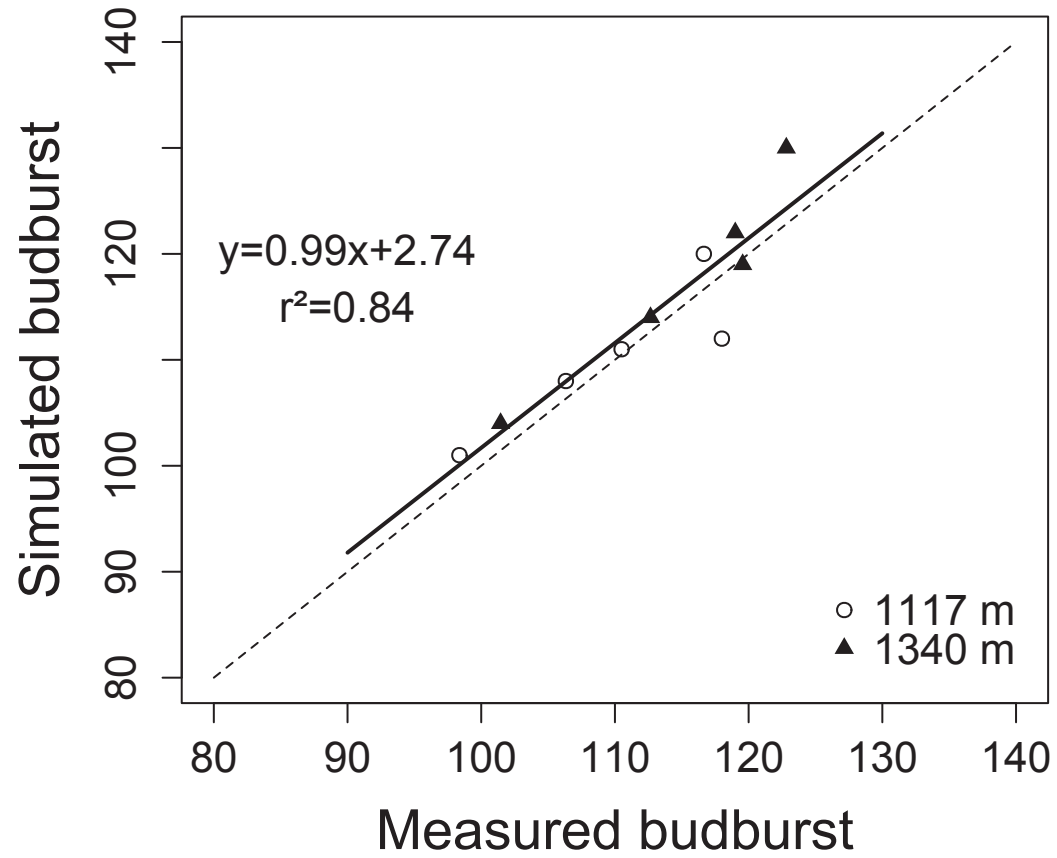
10 **Figure 4:** Change of the temperature sum required for budburst ($C_b - F_{critBB}$) between
11 generations G0 and G5 within populations Alt2 to Alt5 for different scenarios (letter above
12 each graph). The boxplot represents variation across the 21 repetitions. The dashed line
13 correspond to $C_b = 0$ (no change). Population Alt1 was removed because of the low number of
14 surviving individuals at G5.

15 **Figure 5:** Change of the temperature sum required for budburst (F_{critBB}) within generation G0
16 (top panels) and G5 (bottom panels), for scenarios A (neutral, left panels) and B (adaptive
17 evolution, right panels).

18

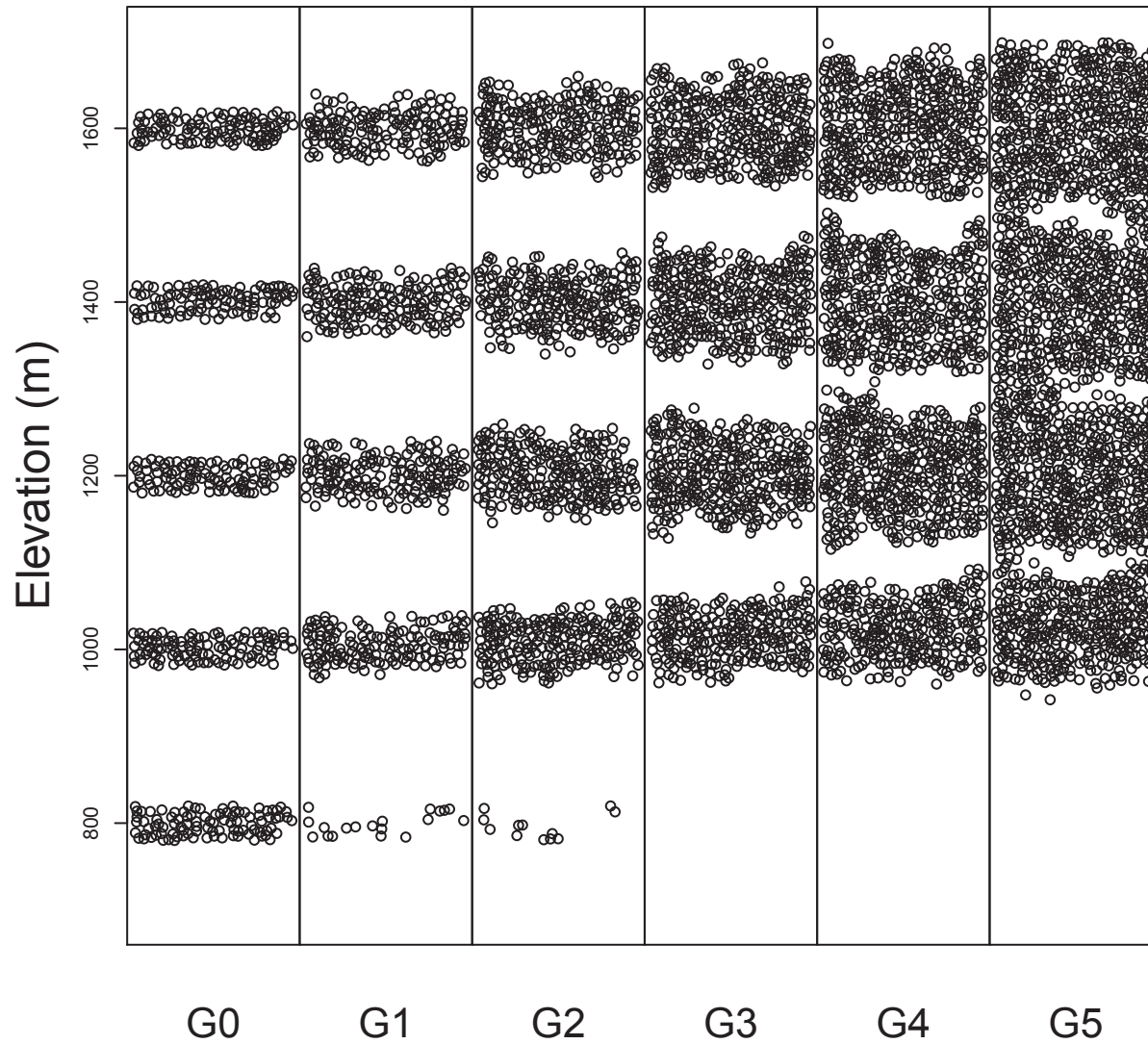
19

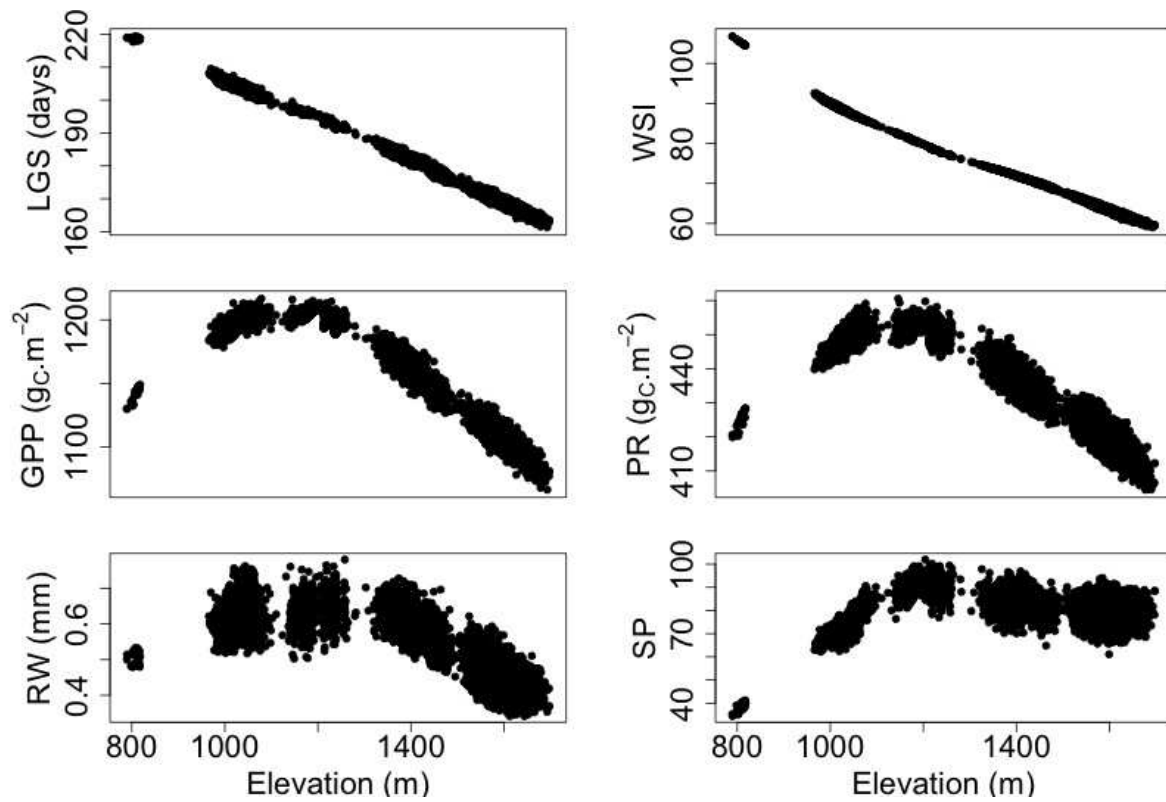
20

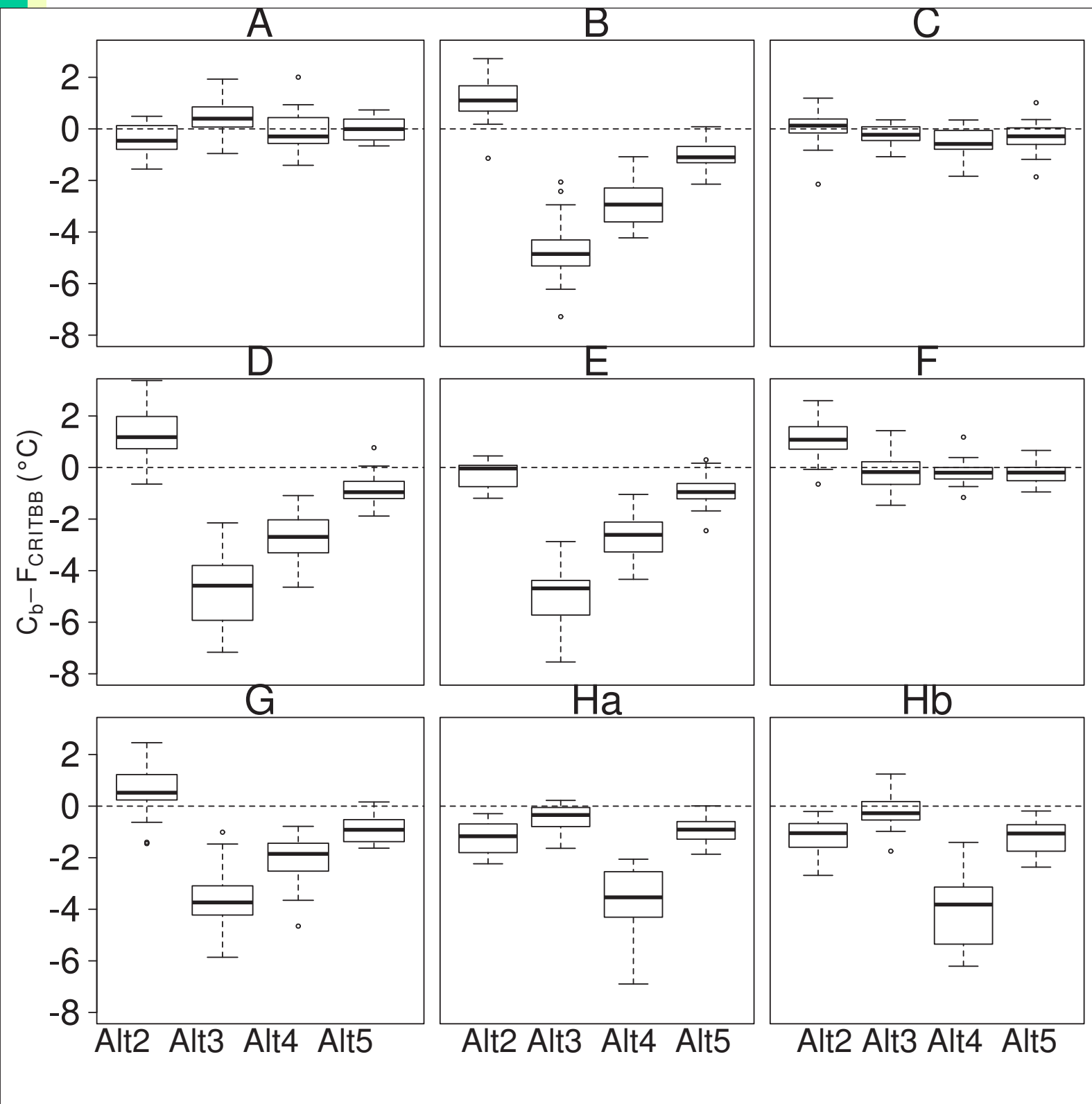


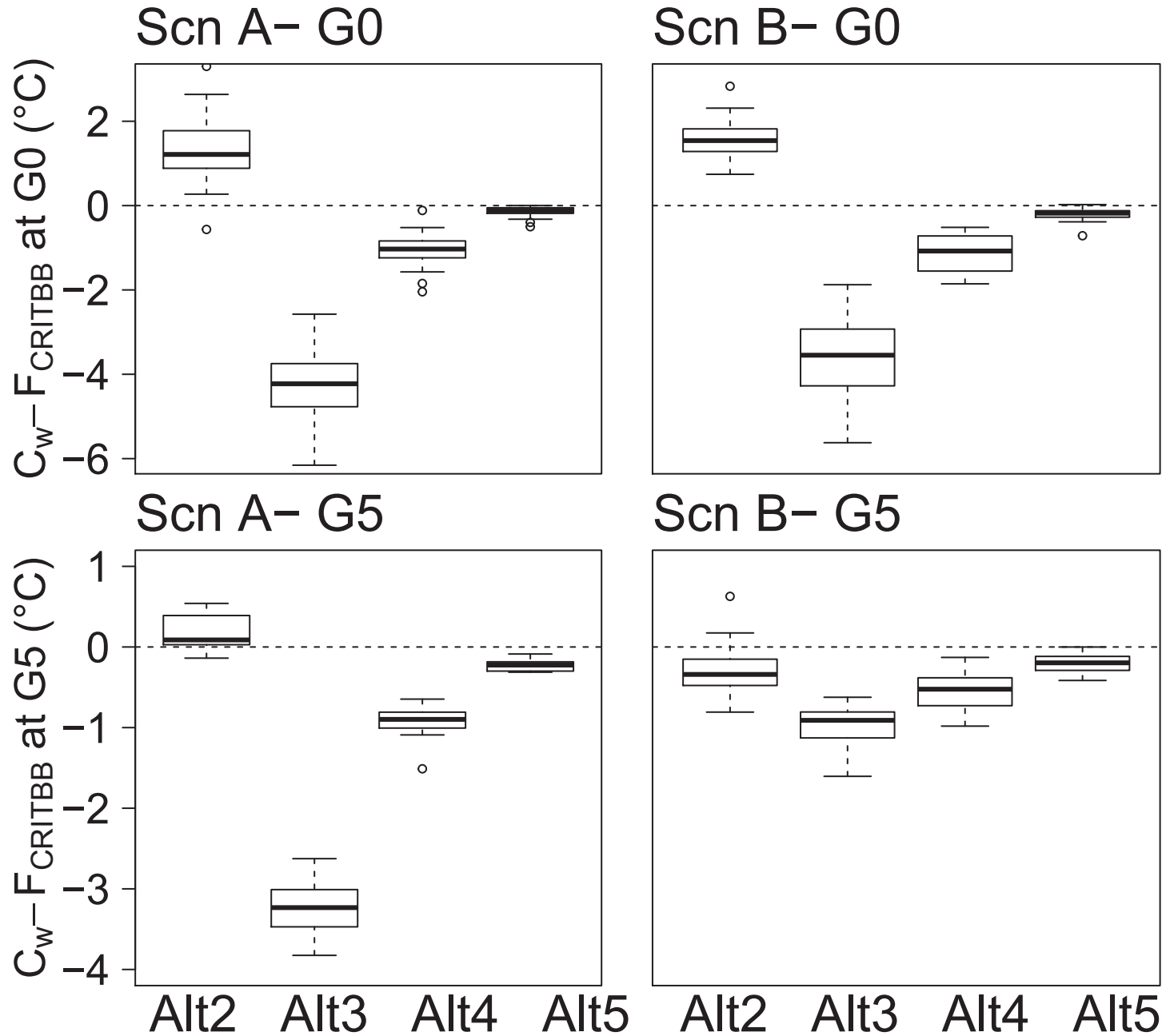
Comment citer ce document :

Oddou-Muratorio, S., Davi, H. (2014). Simulating local adaptation to climate of forest trees with a physio-demo-genetics model. *Evolutionary Applications*, 7 (4), 453–467. DOI : 10.1111/eva.12143









Comment citer ce document :